

# Testing aspherics using two-wavelength holography: use of digital electronic techniques

J. C. Wyant, B. F. Oreb, and P. Hariharan

Two-wavelength holography has been shown to be quite useful for testing aspheric surfaces since it can produce interferograms with a wide range of sensitivities. However, TWH has the drawback that the accuracy attainable from measurements on photographs of the fringes is limited. It is shown how this limitation can be overcome by using digital electronic techniques to evaluate the phase distribution in the interference pattern.

The problem of testing aspheric surfaces is becoming increasingly common in optical fabrication. One solution, which is now well established, is the use of a computer-generated hologram (CGH).<sup>1,2</sup> This has the advantage that once the CGH is made, it can be used to test several identical pieces in a null setup. However, the CGH technique has certain limitations. Without suitable null optics<sup>3</sup> a CGH is limited in the amount of asphericity it can handle. In addition, in the early stages of fabrication, the errors of the test piece may be so large that the interferogram contains too many fringes to permit easy interpretation. Finally, the production of a CGH adds considerably to the cost if only one or two pieces are to be tested.

For these reasons, two-wavelength holography (TWH) has been used as an alternative method for testing aspherics.<sup>4</sup> This technique is much more flexible, since it can produce interferograms with a wide range of sensitivities and is, therefore, most useful in the initial stages of production. However, its use for final tests on an aspheric has the drawback that the accuracy attainable from measurements on photographs of the fringe pattern is limited. This paper shows how this limitation can be overcome by using digital electronic techniques to evaluate the phase distribution in the interference pattern.

The optical system used for these experiments is shown schematically in Fig. 1. The beam from an argon-ion ( $\text{Ar}^+$ ) laser fitted with a wavelength selecting

prism and an intracavity étalon to ensure operation in a single longitudinal mode was divided at an adjustable beam splitter. The two beams obtained were spatially filtered and then expanded in two beam-expanding telescopes to obtain two collimated beams, which were used as the object and reference beams.

The object beam was brought to a focus at the center of curvature of the element under test by lens  $L_1$ . The wave front reflected from this element then returned through the same lens as a collimated beam to the afocal system constituted by  $L_2$  and  $L_3$ , which formed a demagnified image of the pupil of the element under test at  $H$ . An image hologram was recorded on a photothermoplastic coated plate located in this plane, and this hologram was processed *in situ*.

The laser wavelength was then changed from that used to record the hologram (say  $\lambda_1$ ) to a different wavelength (say  $\lambda_2$ ). To obtain an interferogram it is then necessary to readjust the angle of the reference beam so that the object wave reconstructed by the hologram continues to travel in the same direction as the directly transmitted object wave. The need for this adjustment can be avoided in principle if the diffracted beam from a grating with the same spatial frequency as the spatial carrier frequency of the hologram is used as the reference beam. However, this requires a grating of high quality. In addition, errors can be introduced by the lateral displacement of the beam. Accordingly, in the present case this adjustment was made by means of two mirrors  $M_2$  and  $M_3$  in the reference beam path. With these it is possible to reduce both the tilt and the shear to zero.

The interferogram obtained has the same sensitivity as the interferogram that would be obtained if a longer single wavelength  $\lambda_{\text{eq}}$  were used in the interferometer, where

$$\lambda_{\text{eq}} = \lambda_1 \lambda_2 / |\lambda_1 - \lambda_2|. \quad (1)$$

J. C. Wyant is with University of Arizona, Optical Sciences Center, Tucson, Arizona 85721; the other authors are with CSIRO Division of Applied Physics, Sydney, 2070 Australia.

Received 16 April 1984.

0003-6935/84/224020-04\$2.00/0.

© 1984 Optical Society of America.

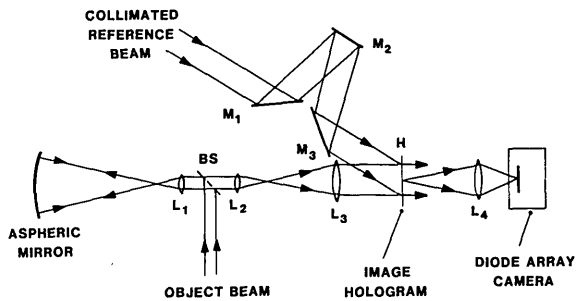


Fig. 1. Optical system used to test aspheric surfaces using two-wavelength holography.

Very rapid and accurate measurements of the phase at a larger number of points over the interferogram were made possible by the use of a digital system.<sup>5,6</sup> The interferogram formed in the hologram plane was imaged by means of a variable-magnification lens  $L_4$  on a  $100 \times 100$  photodiode array, which was coupled through a high-speed 8-bit ADC to a large random-access memory (RAM). This was, in turn, interfaced to a microcomputer which controlled the acquisition of data.

Recording an interferogram involved making three scans of the diode array with the phase of the reference beam shifted for the second and third scans by  $+120^\circ$  and  $-120^\circ$ , respectively. This phase shift was introduced by a mirror in the reference beam path mounted on a piezoelectric translator which was driven by a dc amplifier controlled through a DAC by the microcomputer.

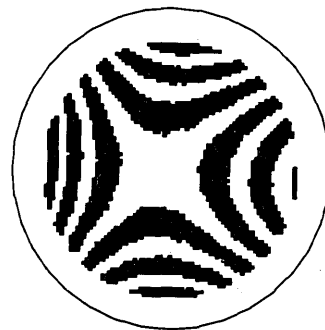
At the end of such a measurement cycle, which takes  $<150$  msec, the RAM contains three readings ( $I_1, I_2, I_3$ ) of the irradiance at each point which are linked to the original phase difference  $\phi$  between the interfering wave fronts at this point by the relation

$$(1/\sqrt{3}) \tan(\phi) = (I_3 - I_2)/(2I_1 - I_2 - I_3). \quad (2)$$

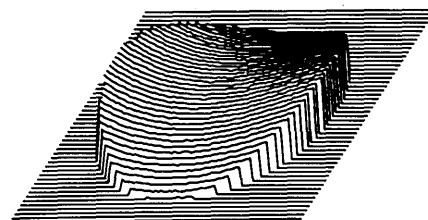
The right-hand side of Eq. (2) is evaluated with 8-bit accuracy by the microcomputer, and values of  $\phi$  are obtained with a nominal accuracy of  $\pm 1^\circ$  from a look-up table. A section of the program compares the values of  $I_1, I_2$ , and  $I_3$  at each point with a preset threshold before calculating the phase and tags all points outside the pupil.

The use of Eq. (2) has the advantage that variations in sensitivity between individual diode elements and nonuniform illumination of the field as well as fixed pattern noise across the detector have a negligible effect on the results.

If the signs of the numerator and denominator of the right-hand side of Eq. (2) are taken into account,  $\phi$  can be determined to a modulus of  $360^\circ$ . If the values of  $\phi$  vary outside this range, an additional processing step is necessary to eliminate discontinuities in the measured wave front before any further processing of the data is undertaken. For this, the values of the phase at neighboring points are examined, and multiples of  $\pm 360^\circ$  are added to the data, where required, to obtain a continuous surface. This presents no problem as long as the phase change between adjacent data points is  $<180^\circ$ .



(A)



(B)

Fig. 2. Contour map and 3-D plot of an aspheric wave front obtained at a wavelength of 488 nm. Contour interval = 0.5 wavelength; maximum deviation from the reference sphere = 2.792 wavelengths.

The first step was to determine the system errors independent of the use of two different wavelengths. For this, a hologram was made of a spherical mirror using the setup shown in Fig. 1 and a wavelength of 488 nm. The spherical mirror was then replaced with an aspheric mirror, and the digital system was used to measure the resulting difference between the wave front stored in the hologram and the wave front produced by the aspheric mirror using the same wavelength. Figure 2 shows typical contour maps and 3-D plots of the resultant wave front. The maximum deviation from the reference sphere was 2.792 wavelengths.

To determine repeatability, the measurements were performed several times, and the difference between pairs of measurements were found point by point. If we exclude a single value of the difference of 0.072 wavelength due to a bad data point, the range of values was 0.031 wavelength, while the rms difference was 0.004 wavelength. These values agree with those obtained in independent measurements using the same digital system with an interferometric setup.<sup>7</sup>

The same aspheric mirror was then tested using two-wavelength holography. A hologram was made using a wavelength of 488 nm, and it was reconstructed using a 514-nm wavelength giving an equivalent wavelength of  $9.47 \mu\text{m}$ . Typical contour maps and 3-D plots are shown in Fig. 3. The average of three data sets at this equivalent wavelength give a maximum deviation from the reference sphere of 0.158 wavelength. Subtracting one data set from another gave an rms difference of 0.004 wavelength. The range of the differences was 0.077 wavelength, essentially due to two bad data points.

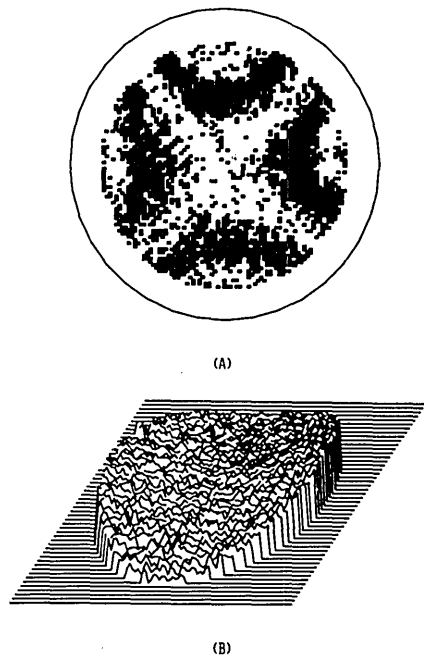


Fig. 3. Contour map and 3-D plot obtained using two-wavelength holography (equivalent wavelength,  $9.47 \mu\text{m}$ ). Contour interval =  $0.05$  wavelength; maximum deviation from a reference sphere =  $0.158$  wavelength.

The results shown in Fig. 3 exhibit an appreciable amount of random spatial noise, probably due to scattered light in the system. This noise can be reduced by averaging the data over a  $3 \times 3$  grid centered on each data point. The smoothed results are shown in Fig. 4.

Since the same aspheric mirror has been tested using single-wavelength and two-wavelength holography, the question is, how well do the two results agree? First, we can compare the values obtained for the deviation from a reference sphere. As shown in Table I, measurements at a single wavelength ( $488 \text{ nm}$ ) gave a value of  $2.792$  wavelengths, while measurements at an equivalent wavelength of  $9.47 \mu\text{m}$  gave a value of  $0.158$  wavelength. The latter corresponds to  $3.066$  wavelengths at  $488 \text{ nm}$ . The difference is  $0.274$  wavelength ( $488 \text{ nm}$ ) or  $0.014$  wavelength ( $9.47 \mu\text{m}$ ).

A more stringent test of the agreement is to take the two data sets and, after proper scaling so both data sets are in the same units, to subtract one from the other point by point. When this was done, the rms difference was  $0.198$  wavelength ( $488 \text{ nm}$ ) or  $0.010$  wavelength ( $9.47 \mu\text{m}$ ), while the range of the differences was  $1.575$  wavelength ( $488 \text{ nm}$ ) or  $0.081$  wavelength ( $9.47 \mu\text{m}$ ). While at first glance these results seem discouraging, after some thought they are reasonable. First, just one bad data point in the two-wavelength data can make the range of the differences look bad. This is especially true because there is a scale factor of  $19.4$  ( $9.47 \mu\text{m}/488 \text{ nm}$ ) between the two data sets. Similarly, while a rms difference of  $0.198$  wavelength ( $488 \text{ nm}$ ) seems large, we have to remember that this corresponds to only  $0.010$  wavelength rms at  $9.47 \mu\text{m}$ . This is only a factor of 2

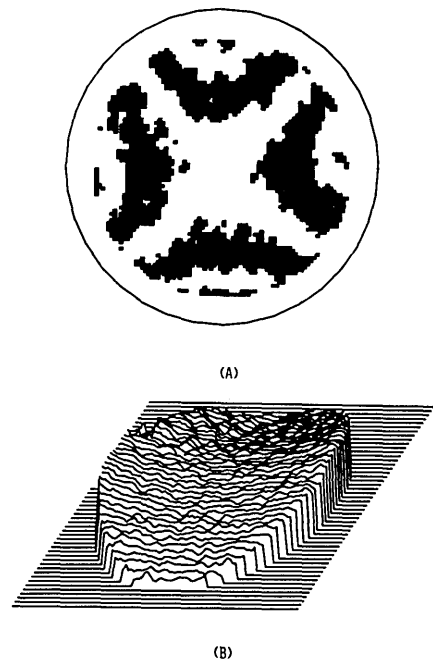


Fig. 4. Contour map and 3-D plot obtained using two-wavelength holography (equivalent wavelength,  $9.47 \mu\text{m}$ ); data averaged over a  $3 \times 3$  grid centered on each point. Contour interval =  $0.05$  wavelength; maximum deviation from a reference sphere =  $0.150$  wavelength.

Table I. Comparison of Values in Wavelengths Obtained for the Deviation of an Aspheric Surface From a Reference Sphere

Single-wavelength measurements		Two-wavelength measurements		Difference	
$488 \text{ nm}$	$9.47 \mu\text{m}$	$488 \text{ nm}$	$9.47 \mu\text{m}$	$488 \text{ nm}$	
$2.792$	$0.158$	$3.066$	$0.014$	$0.274$	

larger than the rms repeatability of  $0.005$  wavelength obtained in measurements at a single wavelength. Thus by using two wavelengths, we are able to extend the dynamic range of the measurement, and the accuracy in units of wavelength is approximately the same for single wavelength measurements and two wavelength measurements.

We believe that the main source of errors in the two-wavelength measurements is changes in the optical paths in the setup between recording the hologram and reconstruction. These changes could be partly due to causes independent of wavelength such as air currents but appear to be largely due to causes linked with the change in the wavelength, such as dispersion in the lenses.

We have also used this technique on surfaces having  $\sim 10$  times the amount of asphericity shown above with very satisfactory results. However, it was difficult to get a good quantitative measure of the accuracy because the deviations from a sphere were too large to measure precisely by conventional interferometry.

These experiments show that measurements can be made by two-wavelength holography (TWH) to a rms repeatability of at least  $1/100$  of the equivalent wavelength if digital electronic techniques are used for the

phase readout. This makes it possible to measure quite large deviations from a sphere with acceptable accuracy, especially for the initial testing of aspheric surface. However, since the actual precision depends on the equivalent wavelength, it is best to keep the equivalent wavelength as short as possible. The main advantage of TWH is that the equivalent wavelength can be selected to suit the amount of asphericity. Since TWH measures the difference between the interference patterns obtained at two different wavelengths, it is important that the setup should be designed to minimize differences resulting from dispersion in the optics or air currents.

The authors thank C. M. Chidley for his skilled assistance in these experiments.

## References

1. A. J. MacGovern and J. C. Wyant, "Computer Generated Holograms for Testing Optical Elements," *Appl. Opt.* **10**, 619 (1971).
2. J. C. Wyant and V. P. Bennett, "Using Computer Generated Holograms to Test Aspheric Wavefronts," *Appl. Opt.* **11**, 2833 (1972).
3. J. C. Wyant and P. K. O'Neill, "Computer Generated Hologram Null Test of Aspheric Wavefronts," *Appl. Opt.* **13**, 2762 (1974).
4. J. C. Wyant, "Testing Aspherics Using Two-Wavelength Holography," *Appl. Opt.* **10**, 2113 (1971).
5. P. Hariharan, B. F. Oreb, and N. Brown, "A Digital Phase Measurement System for Real-Time Holographic Interferometry," *Opt. Commun.* **41**, 393 (1982).
6. P. Hariharan, B. F. Oreb, and N. Brown, "Real-Time Holography Interferometry: A Micro-Computer System for the Measurement of Vector Displacements," *Appl. Opt.* **22**, 876 (1983).
7. P. Hariharan, B. F. Oreb, and A. J. Leistner, "High Precision Digital Interferometry: Its Application to the Production of an Ultrathin Solid Fabry Perot Etalon," *Opt. Eng.* **23**, 294 (1984).
8. J. Schwider, R. Burow, K. E. Elssner, J. Grazanna, R. Spolaczyk, and K. Merkel, "Digital Wave-Front Measuring Interferometry: Some Systematic Error Sources," *Appl. Opt.* **23**, 3421 (1983).

---

## NBS REPORT MAKES IT EASIER TO USE THE MOON FOR MEASURING ANTENNAS

A new publication from the National Bureau of Standards gives simple, precise equations for using the moon as a source for calibrating communication antennas.

Small satellite earth terminals in the 1–10-GHz frequency range can be calibrated for the loss in sensitivity due to noise by comparing noise signals received when the antenna is pointed at the moon with noise signals received when the antenna is pointed away from the moon toward the cold sky. The measurement of primary interest to NBS is the antenna gain-to-system noise temperature ratio (G/T), which is analogous to a measurement of the signal-to-noise ratio of an amplifier.

The NBS system developed to perform G/T measurements is of particular importance to the U.S. Army and its worldwide network of satellite communications facilities. The Army is using the NBS system to measure newly constructed antennas to determine if low-noise specifications have been met and to monitor the performance of orbiting satellites.

The new publication, **An Error Analysis for the Use of Presently Available Lunar Radio Flux Data in Broadbeam Antenna-System Measurements** (TN 1073), gives simple, precise equations for lunar diameter, average brightness temperature, flux density, and shape factor. Flux density is the power per unit area incident on the antenna; shape factor describes how the moon differs from a uniformly radiating disk in terms of the response produced in the antenna. All of these parameters must be factored in to make accurate calibrations using the moon as a noise source.

The flux density and shape factor can be calculated easily for any lunar phase and earth-moon separation distance using the NBS equations and data from the **Astronomical Almanac**. The maximum systematic errors for flux density and shape factor are  $\pm 13\%$  and  $\pm 0.4\%$  respectively for broadbeam antennas in the 1–10-GHz frequency range. The flux density error could be reduced by 3% by taking the variable solar insolation into account. This is the first time that a detailed error analysis has been performed for these parameters.

The 35-page publication is available for \$2 prepaid from the Superintendent of Documents, U.S. Government Printing Office, Washington, D.C. 20402. Order by stock no. 003-003-02555-1.